Eplerenone ameliorates lung fibrosis in unilateral ureteral obstruction rats by inhibiting lymphangiogenesis

ZIQIAN LIU[1,2*], CUIJUAN ZHANG[1,2*], JUAN HAO[2], GEGE CHEN[2], LINGJIN LIU[2], YUNZHAO XIONG[1], YI CHANG[1,3], HUI LI[1,3], TATSUO SHIMOSAWA[4], FAN YANG[1,3] and QINGYOU XU[1,3]

[1]Hebei Key Laboratory of Integrative Medicine on Liver-Kidney Patterns, Institute of Integrative Medicine; [2]Graduate School and [3]College of Integrative Medicine, Hebei University of Chinese Medicine, Shijiazhuang, Hebei 050091, P.R. China; [4]Department of Clinical Laboratory, School of Medicine, International University of Health and Welfare, Narita, Chiba 108-8329, Japan

Received April 28, 2022; Accepted July 18, 2022

DOI: 10.3892/etm.2022.11560

Abstract. Chronic kidney disease (CKD) involves progressive and irreversible loss of renal function, often causing complications and comorbidities and impairing the function of various organs. In particular, lung injury is observed not only in advanced CKD but also in early-stage CKD. The present study investigated the potential involvement of mineralocorticoid receptors (MRs) and lymphatic vessels in lung injury using a 180-day unilateral ureteral obstruction (UUO) model for CKD. Changes in lung associated with lymphangiogenesis and inflammatory were analyzed in UUO rats. The pathology of the lung tissue was observed by hematoxylin and eosin and Masson's staining. Detection of the expression of lymphatic vessel endothelial hyaluronic acid receptor-1 (LYVE-1), Podoplanin, vascular endothelial growth factor receptor-3 (VEGFR-3) and VEGF C to investigate lymphangiogenesis. The mRNA and protein expression levels of IL-1β, monocyte chemotactic protein 1, tumor necrosis factor-α, nuclear factor κB, phosphorylated serum and glucocorticoid-induced protein kinase-1 and MR were evaluated using western blot, reverse transcription-quantitative PCR, immunohistochemical staining and immunofluorescence staining. In the present study, long-term UUO caused kidney damage, which also led to lung inflammation, accompanied by lymphangiogenesis. However, treatment with eplerenone, an MR blocker, significantly reduced the severity of lung injury and lymphangiogenesis. Therefore, lymphangiogenesis contributed to lung fibrosis in UUO rats due to activation of MRs. In addition, transdifferentiation of lymphatic epithelial cells into myofibroblasts may also be involved in lung fibrosis. Collectively, these findings provided a potential mechanism for lung fibrosis in CKD and suggested that the use of eplerenone decreased kidney damage and lung fibrosis.

Correspondence to: Professor Qingyou Xu or Dr Fan Yang, Hebei Key Laboratory of Integrative Medicine on Liver-Kidney Patterns, Institute of Integrative Medicine, Hebei University of Chinese Medicine, 326 Xinshinan Road, Shijiazhuang, Hebei 050091, P.R. China
E-mail: qingyouxu@hebcm.edu.cn
E-mail: yangfanwy@hebcm.edu.cn

*Contributed equally

Abbreviations: CKD, chronic kidney disease; SGK-1, serum- and glucocorticoid-inducible kinase-1; UUO, unilateral ureteral obstruction; RAAS, renin-angiotensin-aldosterone system; LYVE-1, lymphatic vessel endothelial receptor-1; MCP-1, monocyte chemotactic protein 1; α-SMA, α-smooth muscle actin; VEGFR, VEGF receptor

Key words: unilateral ureteral obstruction, lung fibrosis, lymphangiogenesis, eplerenone, mineralocorticoid receptor

Introduction

Chronic kidney disease (CKD) is a key contributor to non-communicable disease morbidity and mortality. In 2017, there were 697.5 million CKD cases worldwide and the prevalence of CKD was estimated to be 9.1% (1). CKD involves progressive, irreversible loss of kidney function, causes complications and comorbidities (2,3), impairs organ function and may lead to premature death. The lungs are severely affected by advanced CKD (4); deterioration of lung function may be associated with fluid retention as well as alterations in metabolism and the endocrine and cardiovascular system (5,6). Moreover, patients with early-stage CKD show changes in lung function (2,7). According to the National Health and Nutrition Examination Survey (2007-2012), lung dysfunction (particularly restrictive lung dysfunction) is associated with degree of impairment of renal function and comorbidities and is an independent predictor of increased mortality in patients with CKD (2,3). Pulmonary fibrosis affects human respiratory function and respiratory function deteriorates with aggravation of lung injury (8). The cellular and molecular mechanisms involved in pulmonary fibrosis have been previously studied. For example, studies on lymphatic vessels in other pathological conditions, such as lung and metastatic cancer, support the potential role of lymphangiogenesis in the pathogenesis of lung fibrosis (9,10). Additionally, lymphangiogenesis is associated with pulmonary destruction and disease severity (11).

Kidney damage activates the renin-angiotensin-aldosterone system (RAAS), which serves a key role in inflammation and fibrosis (12). A previous study reported that activation of mineralocorticoid receptors (MRs) induces macrophage-myofibroblast transition and participates in pulmonary fibrosis in rats that have undergone unilateral ureteral obstruction (UUO) and that this process is attenuated by treatment with selective MR blockers eplerenone (EPL). UUO can cause kidney damage in rats and activate the RAAS system, resulting in aldosterone secretion (13). Aldosterone, as the final effector of RAAS, is involved in occurrence and development of pulmonary inflammation and bleomycin-induced fibrosis (12), however, it is not fully understood whether aldosterone participates in the development of lymphangiogenesis in the lung of UUO rats and the underlying molecular mechanisms remain elusive. The aim of the present study was to investigate the role of aldosterone and MRs activation in pulmonary lymphangiogenesis and whether eplerenone can be used effectively to inhibit lymphangiogenesis.

Materials and methods

Ethical approval of the study protocol. Animal care and experimental protocols were in accordance with the Regulations of the Ministry of Health of the People's Republic of China on Animal Management (documentation no. 55; 2001). All animals received humane care according to Hebei University of Chinese Medicine animal care guidelines (14) and NIH Guidelines for the Care and Use of Laboratory Animals (15). The study was approved by the Animal Protection and Utilization Committee of Hebei University of Chinese Medicine (Shijiazhuang, China; approval no. DWLL2021063).

Model creation, animal grouping and drug administration. Male Wistar rats (n=30; age, ~7 weeks; weight, 170±10 g; cat. no. SCXK 2018-004; Animal Center of Hebei Medical University) were used. Rats had free access to standard chow and tap water at a temperature of 23±2˚C, relative humidity of 60±5% and a 12/12-h light-dark cycle.

After 7 days of acclimatization, the rats were divided randomly into three groups (n=10/group) as follows: Sham, UUO and UUO + EPL (EPL), 10 rats per group. In the sham group, the left ureter was exposed without ligation. In the UUO group, the left ureter was ligated. Following UUO, the rats in the UUO + EPL group were orally administered mixed EPL (1.25 g/kg diet, equivalent to 100 mg eplerenone/kg/day; Pfizer, Inc.). After 180 days, lung tissue was collected for analysis, as described previously (13). For all surgery, rats were anesthetized with isoflurane by continuous inhalation using 3% for induction (4-5 min) and maintained at a concentration of 1.5% during surgery. Every effort was made to alleviate distress of the animals. Rats were sacrificed by cervical dislocation under isoflurane anesthesia. Notably decreased intake of food and water or anuria were defined as humane endpoints for the study.

Histology, immunohistochemistry and immunofluorescence staining. Lungs were harvested and fixed overnight in 4% paraformaldehyde, then dehydrated with 70, 85, 95, 100% anhydrous ethanol for 2 h each, xylene for 15 min, the above steps were all performed at room temperature, then paraffin embedded. Lung sections (thickness, 4 μm) were stained with hematoxylin and eosin (H&E) and Masson's stain. For H&E and Masson's staining, nuclei were stained with hematoxylin for 5 min at 37˚C, 0.5% eosin for 3 min and Ponceau and aniline blue for 5 min, respectively. H&E staining was evaluated using the Ashcroft score (16), and the volume fraction (%) of collagen fibers was analyzed using ImageJ version 1.8.0 (National Institutes of Health). Sections were also used for immunohistochemical staining using antibodies against lymphatic vessel endothelial receptor-1 (LYVE-1; 1:100; cat. no. NB600-1008; Novus Biologicals, LLC), podoplanin (1:100; cat. no. bs-1048R; BIOSS), vascular endothelial growth factor receptor-3 (VEGFR-3; 1:100; cat. no. ab27278; Abcam), serum- and glucocorticoid-inducible kinase-1 (SGK-1; 1:200; cat. no. ab55281; Abcam), interleukin-1β (IL-1β) (1:200; cat. no. ab9722; Abcam), monocyte chemotactic protein 1 (MCP-1; 1:200; cat. no. ab7202; Abcam), tumor necrosis factor-α (TNF-α; 1:100; cat. no. A0277; Abclonal Biotech Co., Ltd.), NF-κB (1:200; cat. no. ab16502; Abcam), α-smooth muscle actin (α-SMA) (1:100; cat. no. bsM-33187M; BIOSS), F4/80 (1:200; cat. no. DF2798; Affinity Biosciences), CD68 (1:200; cat. no. ab283654; Abcam) and collagen I (1:100; cat. no. ab6308; Abcam). Sections were blocked with 10% normal goat serum (cat. no. SP-9002; ZSGB-BIO) for 15 min at 37˚C and primary antibodies were incubated overnight at 4˚C. Finally, sections were incubated at 37˚C with horseradish peroxidase-conjugated secondary antibody (1:200; cat. no. SP-9002; ZSGB-BIO) for 15 min, and use DAB (cat. no. ZLI-9018; ZSGB-BIO) staining solution at room temperature for color development. Sections were observed under a VANOXDM-10AD light photomicrograph device (Olympus Corporation) at x400 or x200 magnification. For immunofluorescence staining, the lungs were perfused, dehydrated in 20 and 30% sucrose solution, frozen in OCT compound and sectioned at a thickness of 6 μm using a freezing microtome. Sections were incubated with monoclonal antibodies against α-SMA, LYVE-1 and VEGFR-3 as aforementioned and then incubated with fluorescein isothiocyanate (FITC; 1:300; cat. no. ab150113; Abcam) and corresponding tetramethylrhodamine isothiocyanate-labeled (TRITC; 1:300; cat. no. ab150078; Abcam) secondary antibody at 37˚C for 2 h. Finally, cell nuclei were stained with 4',6-diamidino-2-phenylindole (cat. no. C0065; Solarbio) at room temperature for 5 min and sections were visualized by confocal laser scanning microscopy using an SP8 system (Leica Microsystems GmbH) at x400 magnification. Positive cells and the staining area were quantified in 10 consecutive high-power fields per lung using ImageJ version 1.8.0 and expressed as the number of positive cells/view or percent positive area.

Western blotting. Total protein from lung tissue was extracted with RIPA lysis buffer (cat. no. BB-3201-100 ml; Bestbio) and protein concentration was determined using bicinchoninic acid kit. The concentration of each histone was adjusted to 5 mg/ml. A total of 8 μl (40 μg) of each histone sample per lane was loaded onto a 10% gel for western blotting and transferred to polyvinylidene difluoride (PVDF) membranes. Following blocking with 5% non-fat milk at room temperature for 2 h, PVDF membranes were incubated overnight at 4˚C with primary antibodies against NF-κB (p65), IL-1β, MCP-1, TNF-α, VEGFR-3,

LYVE-1 (1:500; cat. no. A4352; Abclonal Biotech Co., Ltd.), podoplanin (1:500; cat. no. A13261; Abclonal Biotech Co., Ltd.), VEGF-C (1:500; cat. no. ab9546; Abcam), MR (1:500; cat. no. ab64457; Abcam), phosphorylated-SGK-1 (p-SGK-1; 1:500; cat. no. AF3001; Affinity Biosciences) and GAPDH (1:2,000; cat. no. 60004-1-1 g; ProteinTech, Group, Inc.). The PVDF membranes were incubated with fluorescein-conjugated secondary antibodies (1:20,000; cat. no. D10603-15; LI-COR) for 1 h at room temperature. Protein bands were visualized using Odyssey Infrared Imaging System (LI-COR Biosciences) and protein expression was quantified using ImageJ version 1.8.0 with GAPDH as loading control.

Reverse transcription-quantitative (RT-q)PCR. Total RNA from whole tissue samples was isolated using the EZNA™ Total RNA kit II (Omega Bio-Tek, Inc.). Total RNA was reverse transcribed into cDNA using MonAmp™ ChemoHS qPCR Mix (Monad Biotech Co., Ltd.) according to the manufacturer's instruction. qPCR was performed on the 7500 Fast Real-Time PCR System (Applied Biosystems; ThermoFisher Scientific, Inc.) using SYBR-Green as the detection fluorophore according to the manufacturer's instruction. The thermocycling conditions were as follows: Initial denaturation for 10 min at 95˚C, followed by 40 cycles of 95˚C for 10 sec, 60˚C for 10 sec and 72˚C for 30 sec. The mRNA expression of IL-1β, MCP-1, TNF-α, SGK-1, NF-κB and GAPDH was measured by 7500 Fast Real-Time PCR System using the following primers: IL-1β forward, 5'-GGCAACTGTCCCTGAACTCAAC-3' and reverse, 5'-AAGCTCCACGGGCAAGACATA-3'; MCP-1 forward, 5'-GCTTGGATGACAGAGGCTTGGAG-3' and reverse, 5'-ATTCACAGGTGGCTTGGCTATGAG-3'; TNF-α forward, 5'-CCAGGTTCTCTTCAAGGGACAA-3' and reverse, 5'-GGTATGAAATGGCAAATCGGCT-3'; SGK-1 forward, 5'-CTTCTGTGGCACGCCTGAGTATC-3' and reverse, 5'-AGCCTCTTGGTCCGGTCCTTC-3'; NF-κB forward 5'-TTTTCAGCACTGATTATAGCAGGTT-3' and reverse, 5'-AAGGTATCGCAGTCCCCACC-3' and GAPDH forward, 5'-GTCCATGCCATCACTGCCACTC-3' and reverse, 5'-CGCCTGCTTCACCACCTTCTTG-3'. The primers for MCP-1, NF-κB, SGK-1 and GAPDH were supplied by Sangon Biotech Co., Ltd. The primers for IL-1β and TNF-α were supplied by Wuhan Servicebio Technology Co., Ltd. The mRNA levels were quantified using the $2^{-\Delta\Delta Cq}$ method and normalized to the internal reference gene GAPDH (17).

Statistical analysis. Each experiment was repeated 6 times. Data are presented as the mean ± standard deviation. One-way ANOVA followed by Tukey's post hoc test was used for multiple groups. Tests were performed to determine whether data were normally distributed. Data were analyzed using SPSS version 26.0 (IBM Corp.) and Prism 8.0 (GraphPad Software, Inc.). $P<0.05$ was considered to indicate a statistically significant difference.

Results

UUO-induced lung inflammation and fibrosis are reversed by eplerenone. The present study focused on lung fibrosis in rats that underwent UUO for 180 days. H&E staining showed that UUO caused thickening of alveolar walls and increased infiltration of inflammatory cells, which suggested that long-term UUO induced lung injury (Fig. 1A). Ashcroft score showed that lung damage in the UUO group was more severe than that in the Sham group, while the damage was alleviated following eplerenone treatment. Masson's staining and the collagen volume fraction revealed increased collagen deposition in UUO compared with sham rats, eplerenone mitigated the degree of injury (Fig. 1B). Fibrosis involves accumulation of collagen in the extracellular matrix (18). Collagen I is produced predominantly by myofibroblasts (19,20), which were labeled with α-SMA. Immunostaining of α-SMA and collagen I showed that increased levels of α-SMA and collagen I were associated with UUO and that eplerenone decreased expression of these markers (Fig. 1C-H). These findings suggested that long-term UUO caused kidney damage, which also led to injury and fibrosis in the lung. MR blockade by eplerenone attenuated lung fibrosis in UUO rats, suggesting that MR activation served a role in lung injury.

Eplerenone attenuates UUO-induced lymphangiogenesis in the lung. To investigate if lymphangiogenesis was involved in the lung fibrosis induced by UUO, tissue sections were immunostained with antibodies against lymphatic endothelial cell-specific proteins (e.g. LYVE-1, podoplanin and VEGFR-3). In Sham rats, lymphatic vessels in the lung were present around the airways and large blood vessels, whereas few lymphatic vessels were observed in the lung parenchyma; in UUO rats, lymphatic vessels close to the airways and large blood vessels were enlarged and more lymphatic vessels were present in the lung parenchyma, most of which were in the area infiltrated by inflammatory cells; moreover, lymphangiogenesis was inhibited by eplerenone (Fig. 2A-F). Similar patterns of protein expression were observed for podoplanin, LYVE-1, VEGF-C and VEGFR-3, as indicated by western blotting. The expression of these proteins in the UUO group was significantly higher than in the Sham group, while the expression in the EPL group was significantly lower than in the UUO group (Fig. 2G-K).

These results indicated the underlying pathogenesis of fibrosis in the lungs of UUO rats. Lymphangiogenesis was associated with lung fibrosis and the MR-specific blocker eplerenone mitigated UUO-induced lymphangiogenesis. Hence, MRs may be involved in lymphangiogenesis and lung fibrosis.

MR activation stimulates inflammation and lymphangiogenesis in the lung of UUO rats. Immunostaining showed significant inflammatory cell infiltration in the lung of UUO rats. Compared with sham group, the staining intensity of F4/80 and CD68 in the UUO group was significantly increased, F4/80-positive macrophages and CD68-positive T cells were more widespread in the lung of UUO rats and eplerenone treatment mitigated this change (Fig. 3A and B). The expression levels of MCP-1, IL-1β and TNF-α were compared between Sham and UUO rats. Augmented expression of MCP-1, IL-1β and TNF-α was observed in UUO rats and eplerenone treatment decreased expression of these moieties (Fig. 3C-J). Similar results were obtained by western blotting and RT-qPCR; compared with the Sham group, the expressions of MCP-1, IL-1β and TNF-α were significantly

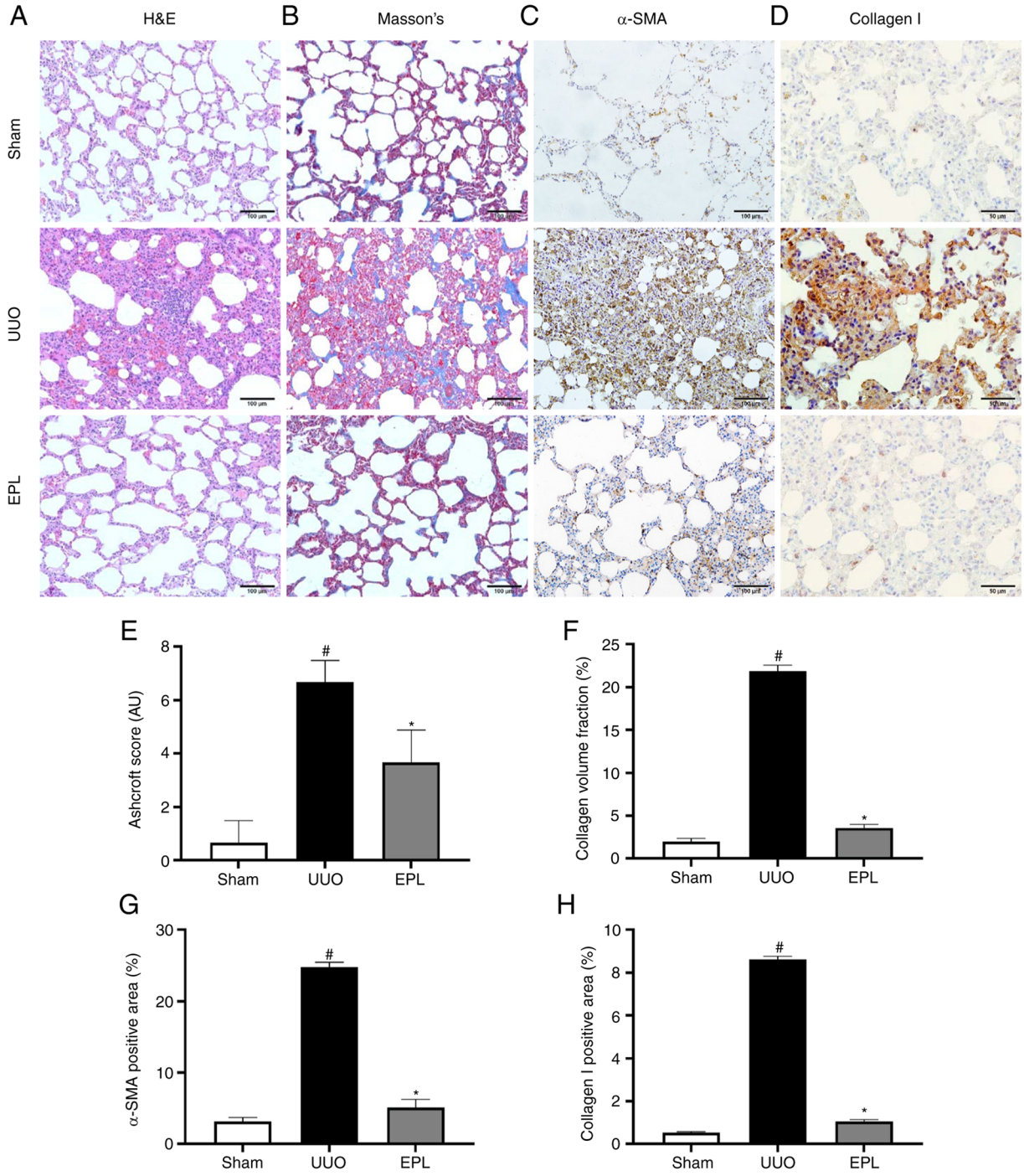

Figure 1. Effect of 180-day UUO and treatment with EPL on lung histology and fibrosis. (A) H&E staining of histological changes in the lung. (B) Masson's staining of fibrosis. (C) Immunohistochemistry staining for α-SMA. Magnification, x200. (D) Immunohistochemistry staining for collagen I. Magnification, x400. (E) Ashcroft score for each group. (F) Collagen volume fraction for each group. (G) α-SMA and (H) collagen I positive expression area. Data are presented as the mean ± standard deviation (n=6). $^{\#}$P<0.05 vs. Sham; *P<0.05 vs. UUO. α-SMA, α-smooth muscle actin; UUO, unilateral ureteral obstruction; H&E, hematoxylin and eosin; EPL, eplerenone.

increased in the UUO group, while EPL decreased their expression (Fig. 3K-Q). The present results indicated that MR activation promoted inflammation in the lung of UUO rats.

To investigate the role of MRs in lung injury, immunohistochemical staining, western blotting and RT-qPCR were performed to identify the downstream molecules of MRs, such as SGK-1, p-SGK-1 and NF-κB. The results showed that compared with the Sham group, the activation of MR enhanced the expression of MR, p-SGK-1/SGK-1 and NF-κB in the UUO group and NF-κB was significantly expressed in the nucleus of the lungs of UUO rats, while EPL significantly decreased expression (Fig. 4). These findings indicated that MR activation was involved in inflammation and lymphangiogenesis in the lung of UUO rats.

MR activation induces endothelial-mesenchymal transition (EndMT) in lung fibrosis. To ascertain if lymphatic endothelial

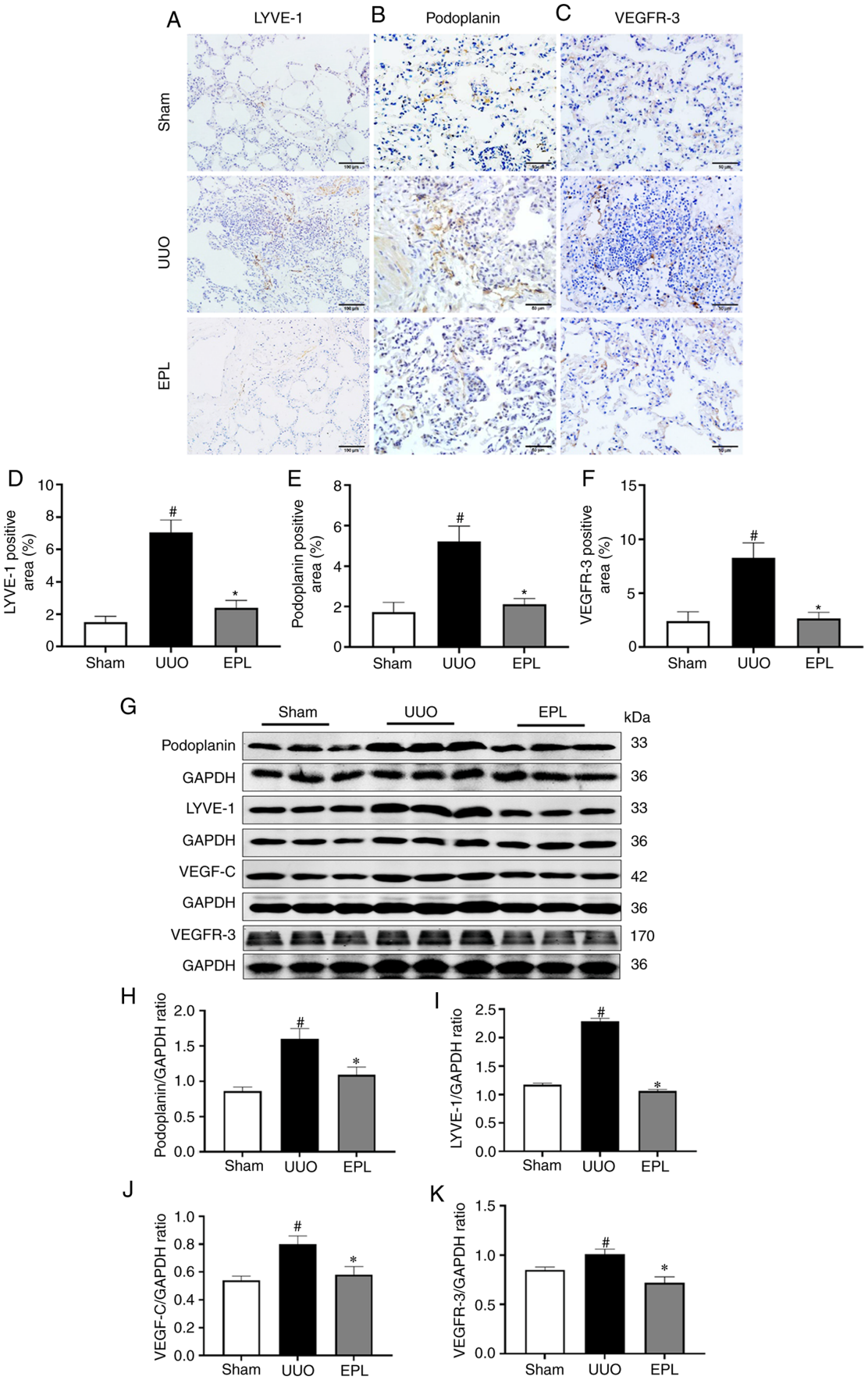

Figure 2. Lymphangiogenesis in the lung of UUO rats. (A) Immunohistochemical staining of lymphatic vessel marker LYVE-1. Magnification, x200. Immunohistochemical staining for (B) podoplanin and (C) VEGFR-3. Magnification, x400. (D) LYVE-1, (E) podoplanin and (F) VEGFR-3 positive expression. (G) Protein expression of podoplanin, LYVE-1, VEGF-C and VEGFR-3 in lung tissue of UUO rats as detected by western blotting. (H) podoplanin, (I) LYVE-1, (J) VEGF-C and (K) VEGFR-3 protein expression. Data are presented as the mean ± standard deviation (n=6). #P<0.05 vs. Sham; *P<0.05 vs. UUO. UUO, unilateral ureteral obstruction; LYVE-1, lymphatic vessel endothelial receptor-1; VEGFR, VEGF receptor; EPL, eplerenone.

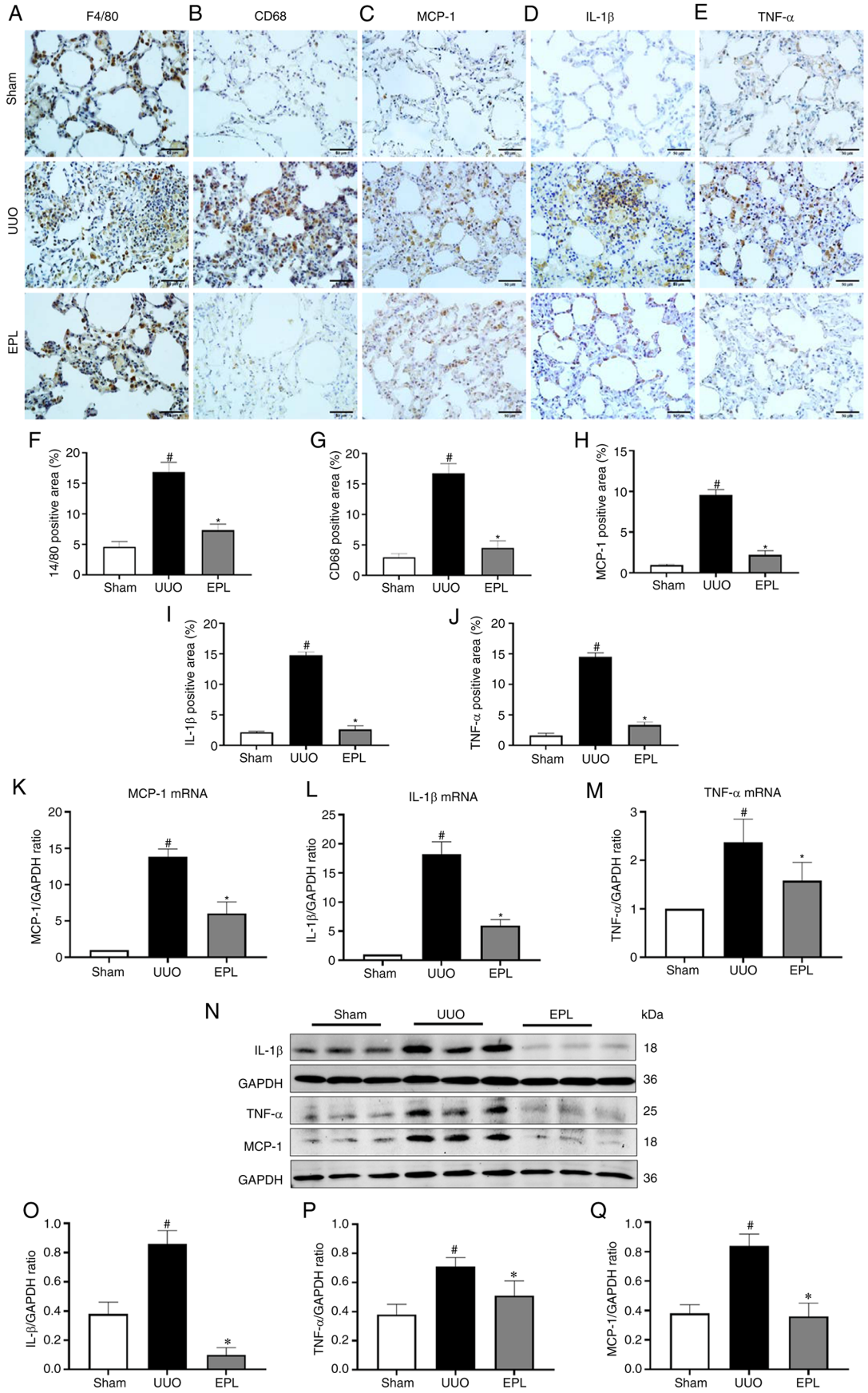

Figure 3. Effect of UUO and EPL on expression of F4/80, CD68, MCP-1, IL-1β and TNF-α in the lung of UUO rats. Immunohistochemical staining of (A) F4/80, (B) CD68, (C) MCP-1, (D) IL-1β and (E) TNF-α. Magnification, x400. (F) F4/80, (G) CD68, (H) MCP-1, (I) IL-1β and (J) TNF-α positive expression area. Expression of (K) MCP-1, (L) IL-1β and (M) TNF-α mRNA as detected by RT-qPCR. (N) Protein expression of IL-1β, TNF-α and MCP-1 as detected by western blotting. (O) IL-1β, (P) TNF-α and (Q) MCP-1 protein expression. Data are presented as the mean ± standard deviation (n=6). #P<0.05 vs. Sham; *P<0.05 vs. UUO. MCP-1, monocyte chemotactic protein 1; UUO, unilateral ureteral obstruction; RT-q, reverse transcription-quantitative; TNF, tumor necrosis factor; EPL, eplerenone.

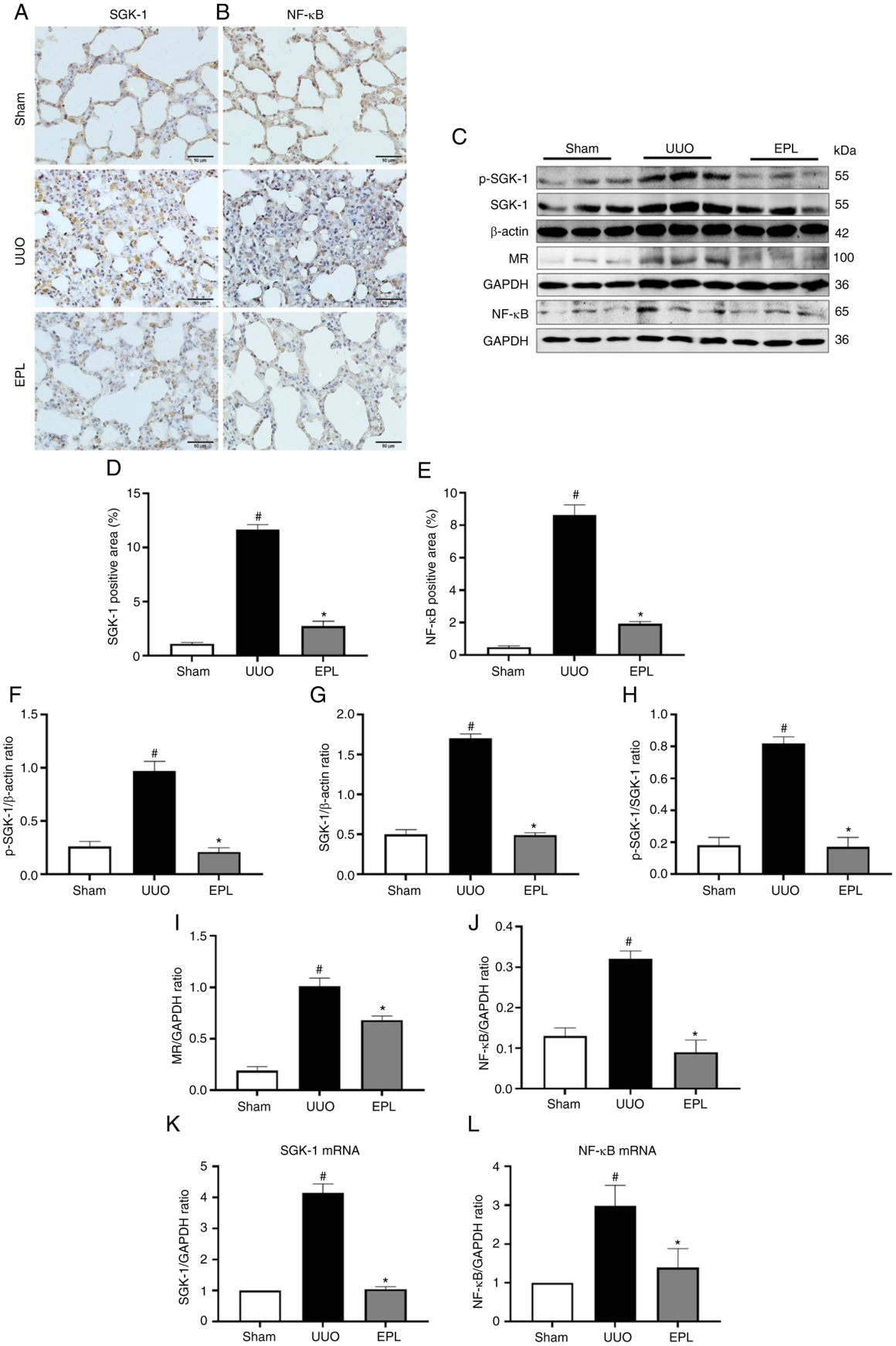

Figure 4. Effect of UUO and EPL on expression of downstream molecules of MRs in lung tissue. Immunohistochemical staining for (A) SGK-1 and (B) NF-κB. Magnification, x400. (C) Protein expression of p-SGK-1, SGK-1, MR and NF-κB as detected by western blotting. (D) SGK-1 and (E) NF-κB positive expression. (F) p-SGK-1 and (G) SGK-1 protein expression in each group. (H) Ratio of p-SGK-1 to SGK-1. (I) MR and (J) NF-κB protein expression. mRNA expression of (K) SGK-1 and (L) NF-κB as detected by RT-qPCR. Data are presented as the mean ± standard deviation (n=6). $^{\#}$P<0.05 vs. Sham; *P<0.05 vs. UUO. UUO, unilateral ureteral obstruction; SGK-1, serum- and glucocorticoid-inducible kinase-1; RT-q, reverse transcription-quantitative; p-, phosphorylated; EPL, eplerenone; MR, mineralocorticoid receptor.

cells were involved in UUO-induced lung fibrosis, immunofluorescent co-staining was performed using specific antibodies against the lymphatic endothelial cell-specific marker LYVE-1 and myofibroblast marker α-SMA. Most lymphatic endothelial cells in the lung of UUO rats co-expressed LYVE-1 and α-SMA, indicating endothelial-myofibroblast transition; this co-staining was attenuated by eplerenone (Fig. 5). Lung samples were stained with antibodies against collagen I, LYVE-1 and α-SMA. The lymphatic vessels of lung tissue co-expressing LYVE-1 and α-SMA were surrounded by collagen I, which indicated that the phenotypic transformation of lymphatic vessels led to production of collagen I (Fig. 6). These results suggested that EndMT promoted fibrosis and pathological changes in the lung of rats that underwent UUO for 180 days. Moreover, MR activation was associated with EndMT.

Discussion

CKD is an important risk factor for development of end-stage renal and lung disease (2,21). Impaired lung function, especially restrictive lung dysfunction, is a common feature of advanced CKD and is associated with severity of renal failure (3). Inflammation is common in patients with CKD and is considered to serve a key role in uremia (22,23). Obstructive kidney disease is one of the primary causes of kidney damage and leads to kidney failure (24). UUO is a classic model used to study obstructive kidney disease and renal fibrosis (25-27). In 180-day UUO rats, UUO caused kidney injury and systemic blood pressure changes. Although the renal function damage in this model is not serious, the heart and lungs can be damaged, lung fibrosis may appear and eplerenone improves the condition (13).

A previous study showed that inflammatory cell infiltration occurs in UUO-induced lung fibrosis, macrophages participate in the development of lung fibrosis via macrophage-myofibroblast transition and MR blockers protect the lung from chronic damage and fibrosis (13). The present study confirmed these previous findings by showing extensive lung interstitial damage in UUO rats, pronounced α-SMA expression and collagen deposition, which reflect the presence of activated myofibroblasts associated with inflammation. This was evidenced by increased infiltration of inflammatory cells (F4/80-positive macrophages and CD68-positive T cells) and release of proinflammatory factors (MCP-1, IL-1β and TNF-α) compared with Sham rats. Moreover, lung injury was ameliorated by eplerenone. Additionally, new lymphatic vessels were found in the lung tissue of UUO rats. Therefore, the present study focused on the role of lymphangiogenesis in lung inflammation and fibrosis in UUO rats.

Lymphatic vessels contribute to human diseases such as cardiovascular disease (28), renal fibrosis (29), interstitial lung disease (30), cancer metastasis (31) and inflammatory bowel disease (32). The features of chronic inflammation include lymphangiogenesis and blood vessel remodeling (33). Lymphangiogenesis induced by macrophages and granulocytes typically occurs at sites of tissue inflammation, which leads to production of large amounts of VEGF-C. VEGF-C upregulation stimulates lymphangiogenesis and VEGF-C is induced in response to proinflammatory cytokines (such as TNF-α), potentially by activating the NF-κB pathway (34). VEGF-C induces lymphangiogenesis primarily by combining directly with VEGFR-3, which is expressed on lymphatic endothelial cells (21). Studies have shown that lymphatic vasculature changes in almost all lung disease and lymphatic endothelial cell-specific proteins (such as LYVE-1, podoplanin, VEGFR-3) have been investigated in previous studies (9,11,35). In the present study, lymphangiogenesis was observed in the lung parenchyma. Most lymphatic vessels were in areas infiltrated by inflammatory cells and the secretion of proinflammatory cytokines was increased significantly. The present results demonstrated the involvement of VEGF-C and inflammatory cytokines in the UUO rat model.

Lymphangiogenesis has been studied in airway and interstitial lung disease and is associated with tissue repair (30). Lymphangiogenesis is also present in lung fibrosis, which is associated with disease severity (30,36). Immunohistochemical assessment with monoclonal antibodies against LYVE-1, podoplanin and VEGFR-3 showed an increased number of lymphatic vessels in the lung of UUO rats. Simultaneously, accumulation of inflammatory cells such as macrophages in proximity to lymphatic vessels and increased levels of proinflammatory factors such as MCP-1, IL-1β and TNF-α in lung tissue were observed. Inflammation is a potent inducer of lymphangiogenesis (37). Proinflammatory factors such as IL-1 and TNF-α induce upregulation of VEGF-C expression (38). Therefore, it was hypothesized that the association between inflammation and lymphatics, both of which promote fibrosis and lymphangiogenesis, were directly activated by inflammatory cells via production of proinflammatory factors. Lymphangiogenesis and inflammation are interdependent processes that promote progression of lung damage and fibrosis (11,33). A previous study showed that the length density of lymphatic vessels (vessel length per μm^3 tissue) is correlated with histopathological components of tissue fibrosis, namely organizing and fibrotic collagen, in usual and non-specific interstitial pneumonia (39). In the present study, only the positive areas of lymphatic vessels were quantified, whereas the length density was not measured.

The present study showed that MRs participate directly in lymphangiogenesis in the lung tissue of UUO rats. Long-term UUO in rats leads to increased levels of aldosterone in plasma. This leads to MR activation, accumulation of inflammatory cells and release of proinflammatory factors in the lung (13). Vicenzi *et al* (40) showed that RAAS and the final effector (aldosterone) may be responsible for inflammation and oxidative damage to organs such as heart and lung. Inappropriate activation of RAAS adversely influences several diseases including diabetic nephropathy (41) and hypertension (42), while drugs that attenuate RAAS, such as angiotensin-converting-enzyme inhibitor and angiotensin receptor and MR blockers, are useful for hypertension, left ventricular dysfunction, acute myocardial infarction, diabetic nephropathy and atherosclerosis (12) and also attenuate pathological pulmonary vascular involved in pulmonary arterial hypertension and right ventricular heart failure (43). MR blockers prevent cardiovascular disease by decreasing vascular inflammation and injury, endothelial dysfunction and myocardial fibrosis; their role in respiratory system disease is also associated with broad-spectrum anti-inflammatory activity (12). The augmented level of

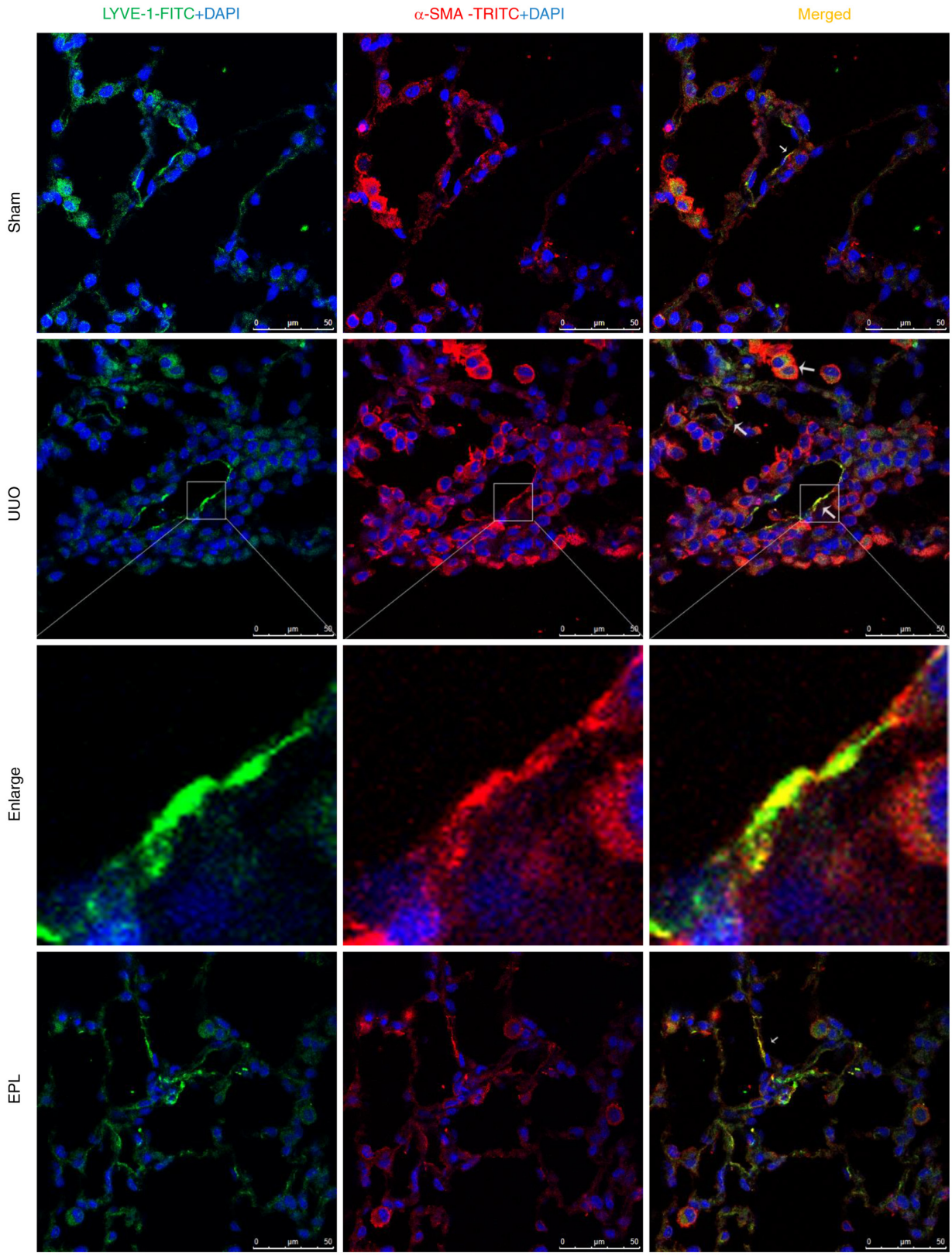

Figure 5. EndMT in the lung of UUO rats. Co-expression of lymphatic vessel (LYVE-1, green) and myofibroblast (α-SMA, red) markers was detected by two-color immunofluorescence staining and indicated EndMT. Magnification, x400. Representative image of LYVE-1 $^{+}$/α-SMA $^{+}$ EndMT cells is magnification, x8. Nuclei were stained blue with DAPI. UUO, unilateral ureteral obstruction; EndMT, endothelial-mesenchymal transition; LYVE-1, lymphatic vessel endothelial receptor-1; α-SMA, α-smooth muscle actin; EPL, eplerenone.

proinflammatory biomarkers was associated with higher aldosterone level (12) and inflammation is associated with proliferation and remodeling of lymphatic vessels (37,44). Therefore, it was hypothesized in this study that UUO-induced lymphangiogenesis may be associated with activation of MRs (receptors of aldosterone). A common pathway by which

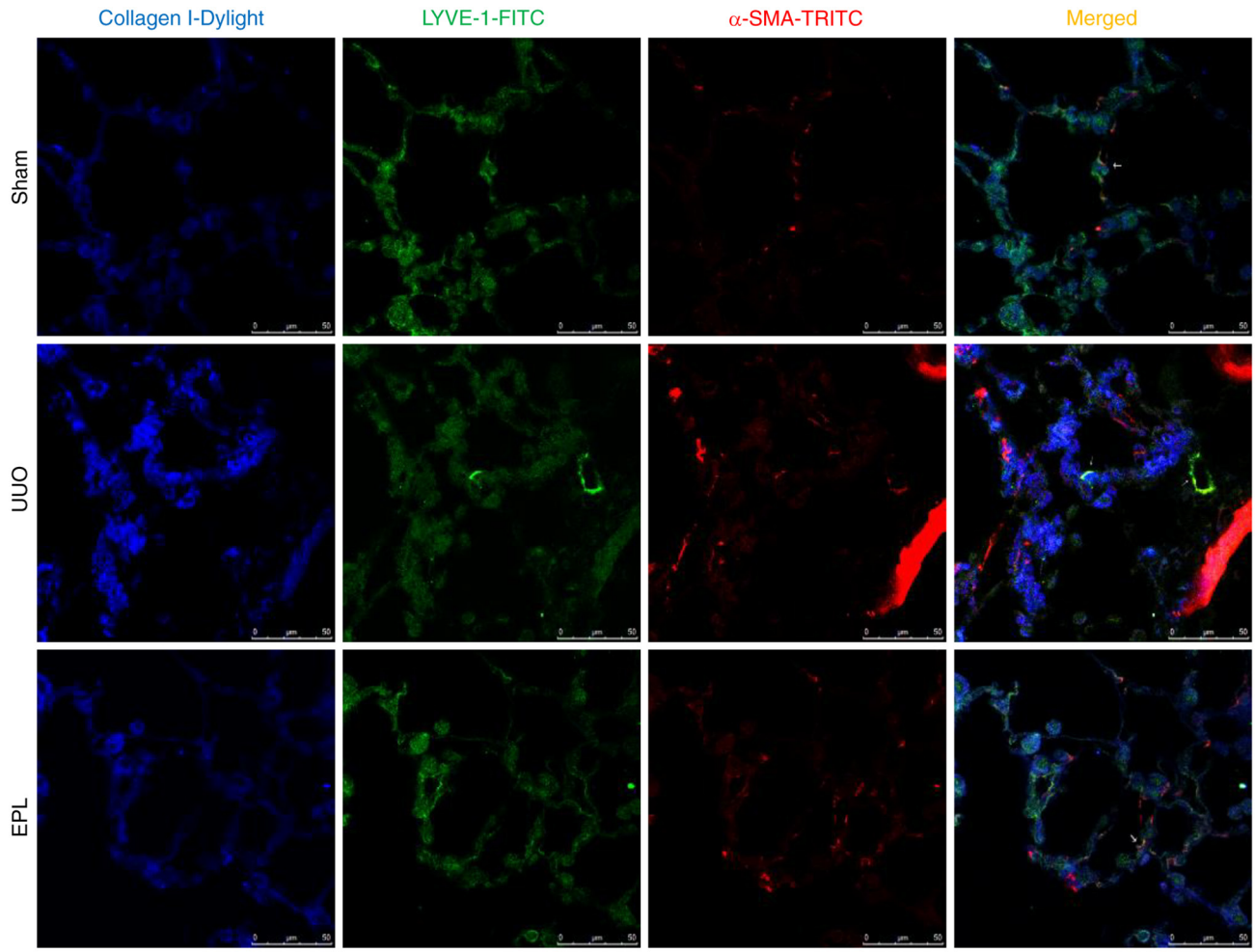

Figure 6. Cells undergoing endothelial-mesenchymal transition produce collagen in the lung tissue of UUO rats. Three-color confocal laser scanning microscopy of cells co-expressing LYVE-1 (green), α-SMA (red) and collagen I (blue). Lymphatic vessels co-expressing LYVE-1 and α-SMA are surrounded by collagen I. Magnification, x400. LYVE-1, lymphatic vessel endothelial receptor-1; α-SMA, α-smooth muscle actin; UUO, unilateral ureteral obstruction; EPL, eplerenone.

proinflammatory cytokines trigger lymphangiogenesis is the NF-κB pathway, which induces VEGF expression (45). NF-κB-mediated VEGF expression is also induced by other molecules or conditions. For example, lipopolysaccharide increases VEGF-C release in colorectal cancer via the TLR4-NF-κB/JNK pathway (46). Nuclear receptor subfamily 3 group C member 2 is a nuclear horsmone receptor of the proteinase 3C class and encodes MR. When aldosterone binds to MR, the aldosterone-MR complex translocates to the nucleus and regulates NaCl and water homeostasis, while also activating target genes such as ENaC (47). In the present study, increased expression of NF-κB, SGK-1 and p-SGK-1 in the UUO group was reversed by eplerenone, demonstrating that MR induced NF-κB activation. Aldosterone receptor blocker spironolactone decreases pulmonary inflammation induced by bleomycin and lipopolysaccharide (48,49). These findings also support the present results and the role of aldosterone in lung inflammation and lung fibrosis. Moreover, the MR blocker eplerenone attenuated lung inflammation and lymphangiogenesis in UUO rats.

Myofibroblasts are key effector cells involved in organ fibrosis by continuously accumulating and contracting scar tissue beyond normal repair. Myofibroblasts are the primary collagen-producing cell type during fibrosis, but their origin remains unclear. Evidence suggests that myofibroblasts have multiple cellular origins, including bone marrow-derived fibrocytes and fibroblasts (50). Lymphangiogenesis under pathological conditions leads to an increase in number of lymphatic vessels and proliferation of lymphatic endothelial cells (9). A recent study suggested that lymphatic endothelial cells heterogeneous and multifunctional under physiological conditions, tumor exposed-lymphatic endothelial cells may exert fibroblast-like properties' by secreting tumor-promoting factors (51). Studies have shown that increased number of lymphatic vessels correlates with the degree of tissue damage, and is associated with fibrosis (21,52). TGF-β2-treated human skin-derived lymphatic endothelial cells (HDLECs) show increased expression of smooth muscle protein 22-α, a mesenchymal cell marker, and TNF-α enhances this, suggesting that HDLECs undergo EndMT (53). A recent study demonstrated that human lymphatic endothelial cells (hLECs) express vimentin and α-SMA upon stimulation with aldosterone and eplerenone inhibits this co-expression, suggesting that hLECs are involved in cardiac fibrosis via EndMT (14). In the present study, lymphatic endothelial cells in the lung of UUO rats also underwent phenotypic transformation, becoming

myofibroblast-like cells and secreting collagen to participate in lung fibrosis.

One limitation to this study is the lack of observation at multiple time points. The present study only tested indicators after 180 days of modeling; future studies should investigate the dynamic changes in the lung during this process in UUO models of different durations, for example 90 and 120 days. Moreover, future studies should investigate changes in density and contractility of lymphatic vessels and examine whether organelles of lymphatic endothelial cells are damaged to verify the function of lymphatic vessels. Further studies are needed to clarify the mechanism by which eplerenone attenuates long-term UUO-induced lung fibrosis by inhibiting inflammation. The present immunostaining results revealed higher macrophage and T cell accumulation in the lung. However, the role of these cells in release of proinflammatory factors remains unclear. Therefore, further investigation is required to determine the precise molecular mechanisms by which MR promotes lymphangiogenesis using both *in vivo* and *in vitro* studies.

In conclusion, the present results suggested a novel mechanism by which lymphangiogenesis participates in the pathogenesis of UUO-induced lung fibrosis. UUO-induced kidney injury increased aldosterone release, which led to activation of MR in the lung and enhancement of inflammation and lymphangiogenesis, resulting in lung damage and fibrosis. The mechanism identified in the present study not only adds to understanding of the pathogenesis of lung injury in patients with CKD but also provides a potential novel therapeutic target for anti-lung fibrosis medications based on crosstalk between the kidney and lung.

Acknowledgements

Not applicable.

Funding

The present study was supported by the Natural Science Foundation of China (grant nos. 82174317 and 81873251), Science and Technology Projects of Hebei Education Department (grant no. QN2020116), Outstanding Young Teachers Basic Research Program of Hebei University of Chinese Medicine (grant no. YQ2020007) and Construction Program of New research and Development Platform and Institution, Hebei Province Innovation Ability Promotion Plan (grant no. 20567624H).

Availability of data and materials

The datasets used and/or analyzed during the current study are available from the corresponding author on reasonable request.

Authors' contributions

ZL, CZ, JH, GC and LL performed the experiments, collected data and wrote the manuscript. YX, YC, HL, FY, TS and QX analyzed the data and wrote the manuscript. FY, TS and QX confirm the authenticity of all the raw data. All authors have read and approved the final manuscript.

Ethics approval and consent to participate

The present study protocol was approved by the Ethics Committee of Hebei University of Chinese Medicine (approval no. DWLL2021063).

Patient consent for publication

Not applicable.

Competing interests

The authors declare that they have no competing interests.

References

1. GBD Chronic Kidney Disease Collaboration: Global, regional, and national burden of chronic kidney disease, 1990-2017: A systematic analysis for the global burden of disease study 2017. Lancet 395: 709-733, 2020.
2. Mukai H, Ming P, Lindholm B, Heimbürger O, Barany P, Stenvinkel P and Qureshi AR: Lung dysfunction and mortality in patients with chronic kidney disease. Kidney Blood Press Res 43: 522-535, 2018.
3. Navaneethan SD, Mandayam S, Arrigain S, Rahman M, Winkelmayer WC and Schold JD: Obstructive and restrictive lung function measures and CKD: National health and nutrition examination survey (NHANES) 2007-2012. Am J Kidney Dis 68: 414-421, 2016.
4. Faria Rde S, Fernandes N, Lovisi JC, Reboredo Mde M, Marta MS, Pinheiro Bdo V and Bastos MG: Pulmonary function and exercise tolerance are related to disease severity in pre-dialytic patients with chronic kidney disease: A cross-sectional study. BMC Nephrol 14: 184, 2013.
5. Salerno FR, Parraga G and McIntyre CW: Why is your patient still short of breath? Understanding the complex pathophysiology of dyspnea in chronic kidney disease. Semin Dial 30: 50-57, 2017.
6. Mukai H, Ming P, Lindholm B, Heimbürger O, Barany P, Anderstam B, Stenvinkel P and Qureshi AR: Restrictive lung disorder is common in patients with kidney failure and associates with protein-energy wasting, inflammation and cardiovascular disease. PLoS One 13: e0195585, 2018.
7. Lelii M, Senatore L, Paglialonga F, Consolo S, Montini G, Rocchi A, Marchisio P and Patria MF: Respiratory complications and sleep disorders in children with chronic kidney disease: A correlation often underestimated. Paediatr Respir Rev: S1526-0542(22)00008-2, 2022 (Epub ahead of print).
8. Plantier L, Cazes A, Dinh-Xuan AT, Bancal C, Marchand-Adam S and Crestani B: Physiology of the lung in idiopathic pulmonary fibrosis. Eur Respir Rev 27: 170062, 2018.
9. Gaje PN, Stoia-Djeska I, Cimpean AM, Ceausu RA, Tudorache V and Raica M: Lymphangiogenesis as a prerequisite in the pathogenesis of lung fibrosis. In Vivo 28: 367-373, 2014.
10. Suzuki H, Kaneko MK and Kato Y: Roles of podoplanin in malignant progression of tumor. Cells 11: 575, 2022.
11. Glasgow CG, El-Chemaly S and Moss J: Lymphatics in lymphangioleiomyomatosis and idiopathic pulmonary fibrosis. Eur Respir Rev 21: 196-206, 2012.
12. Lieber GB, Fernandez X, Mingo GG, Jia Y, Caniga M, Gil MA, Keshwani S, Woodhouse JD, Cicmil M, Moy LY, *et al*: Mineralocorticoid receptor antagonists attenuate pulmonary inflammation and bleomycin-evoked fibrosis in rodent models. Eur J Pharmacol 718: 290-298, 2013.
13. Yang F, Chang Y, Zhang C, Xiong Y, Wang X, Ma X, Wang Z, Li H, Shimosawa T, Pei L and Xu Q: UUO induces lung fibrosis with macrophage-myofibroblast transition in rats. Int Immunopharmacol 93: 107396, 2021.
14. Chen G, Chang Y, Xiong Y, Hao J, Liu L, Liu Z, Li H, Qiang P, Han Y, Xian Y, *et al*: Eplerenone inhibits UUO-induced lymphangiogenesis and cardiac fibrosis by attenuating inflammatory injury. Int Immunopharmacol 108: 108759, 2022.

15. National Research Council (US) Committee for the Update of the Guide for the Care and Use of Laboratory Animals: Guide for the care and use of laboratory animals. 8th edition. Washington (DC): National Academies Press (US), 2011.
16. Ashcroft T, Simpson JM and Timbrell V: Simple method of estimating severity of pulmonary fibrosis on a numerical scale. J Clin Pathol 41: 467-470, 1988.
17. Livak K and Schmittgen T: Analysis of relative gene expression data using real-time quantitative PCR and the 2(-Delta Delta C(T)) method. Methods 25: 402-408, 2001.
18. Karsdal MA, Nielsen SH, Leeming DJ, Langholm LL, Nielsen MJ, Manon-Jensen T, Siebuhr A, Gudmann NS, Rønnow S, Sand JM, *et al*: The good and the bad collagens of fibrosis-their role in signaling and organ function. Adv Drug Deliv Rev 121: 43-56, 2017.
19. Luchsinger LL, Patenaude CA, Smith BD and Layne MD: Myocardin-related transcription factor-A complexes activate type I collagen expression in lung fibroblasts. J Biol Chem 286: 44116-44125, 2011.
20. Chen Y, Kim J, Yang S, Wang H, Wu CJ, Sugimoto H, LeBleu VS and Kalluri R: Type I collagen deletion in αSMA^{+} myofibroblasts augments immune suppression and accelerates progression of pancreatic cancer. Cancer Cell 39: 548-565.e6, 2021.
21. Tanabe K, Wada J and Sato Y: Targeting angiogenesis and lymphangiogenesis in kidney disease. Nat Rev Nephrol 16: 289-303, 2020.
22. Girndt M, Trojanowicz B and Ulrich C: Monocytes in uremia. Toxins (Basel) 12: 340, 2020.
23. Glorieux G, Cohen G, Jankowski J and Vanholder R: Platelet/leukocyte activation, inflammation, and uremia. Semin Dial 22: 423-427, 2009.
24. Stevens S: Obstructive kidney disease. Nurs Clin North Am 53: 569-578, 2018.
25. Xiong Y, Chang Y, Hao J, Zhang C, Yang F, Wang Z, Liu Y, Wang X, Mu S and Xu Q: Eplerenone attenuates fibrosis in the contralateral kidney of UUO rats by preventing macrophage-to-myofibroblast transition. Front Pharmacol 12: 620433, 2021.
26. Bai Y, Wang W, Yin P, Gao J, Na L, Sun Y, Wang Z, Zhang Z and Zhao C: Ruxolitinib alleviates renal interstitial fibrosis in UUO mice. Int J Biol Sci 16: 194-203, 2020.
27. Chaabane W, Praddaude F, Buleon M, Jaafar A, Vallet M, Rischmann P, Galarreta CI, Chevalier RL and Tack I: Renal functional decline and glomerulotubular injury are arrested but not restored by release of unilateral ureteral obstruction (UUO). Am J Physiol Renal Physiol 304: F432-F439, 2013.
28. Balasubbramanian D and Mitchell BM: Lymphatics in cardiovascular physiology. Cold Spring Harb Perspect Med: a041173, 2022 (Epub ahead of print).
29. Xu G: Renal interstitial lymphangiogenesis in renal fibrosis. Adv Exp Med Biol 1165: 543-555, 2019.
30. Yamashita M: Lymphangiogenesis and lesion heterogeneity in interstitial lung diseases. Clin Med Insights Circ Respir Pulm Med 9 (Suppl 1): S111-S121, 2016.
31. Diao X, Guo C and Li S: Progress in the mechanism of lymphangiogenesis and lymphatic metastasis of non-small cell lung cancer. Zhongguo Fei Ai Za Zhi 24: 874-880, 2021 (In Chinese).
32. Ocansey DKW, Pei B, Xu X, Zhang L, Olovo CV and Mao F: Cellular and molecular mediators of lymphangiogenesis in inflammatory bowel disease. J Transl Med 19: 254, 2021.
33. Nihei M, Okazaki T, Ebihara S, Kobayashi M, Niu K, Gui P, Tamai T, Nukiwa T, Yamaya M, Kikuchi T, *et al*: Chronic inflammation, lymphangiogenesis, and effect of an anti-VEGFR therapy in a mouse model and in human patients with aspiration pneumonia. J Pathol 235: 632-645, 2015.
34. Tammela T and Alitalo K: Lymphangiogenesis: Molecular mechanisms and future promise. Cell 140: 460-476, 2010.
35. Stump B, Cui Y, Kidambi P, Lamattina AM and El-Chemaly S: Lymphatic changes in respiratory diseases: More than just remodeling of the lung? Am J Respir Cell Mol Biol 57: 272-279, 2017.
36. Kropski JA, Richmond BW, Gaskill CF, Foronjy RF and Majka SM: Deregulated angiogenesis in chronic lung diseases: A possible role for lung mesenchymal progenitor cells (2017 Grover Conference Series). Pulm Circ 8: 2045893217739807, 2018.
37. Buttler K, Lohrberg M, Gross G, Weich HA and Wilting J: Integration of CD45-positive leukocytes into newly forming lymphatics of adult mice. Histochem Cell Biol 145: 629-636, 2016.
38. Cha HS, Bae EK, Koh JH, Chai JY, Jeon CH, Ahn KS, Kim J and Koh EM: Tumor necrosis factor-alpha induces vascular endothelial growth factor-C expression in rheumatoid synoviocytes. J Rheumatol 34: 16-19, 2007.
39. Lara AR, Cosgrove GP, Janssen WJ, Huie TJ, Burnham EL, Heinz DE, Curran-Everett D, Sahin H, Schwarz MI, Cool CD, *et al*: Increased lymphatic vessel length is associated with the fibroblast reticulum and disease severity in usual interstitial pneumonia and nonspecific interstitial pneumonia. Chest 142: 1569-1576, 2012.
40. Vicenzi M, Ruscica M, Iodice S, Rota I, Ratti A, Di Cosola R, Corsini A, Bollati V, Aliberti S and Blasi F: The efficacy of the mineralcorticoid receptor antagonist canrenone in COVID-19 patients. J Clin Med 9: 2943, 2020.
41. Ambinathan JPN, Sridhar VS, Lytvyn Y, Lovblom LE, Liu H, Bjornstad P, Perkins BA, Lovshin JA and Cherney DZI: Relationships between inflammation, hemodynamic function and RAAS in longstanding type 1 diabetes and diabetic kidney disease. J Diabetes Complications 35: 107880, 2021.
42. Ferrari R: RAAS inhibition and mortality in hypertension. Glob Cardiol Sci Pract 2013: 269-278, 2013.
43. Boehm M, Arnold N, Braithwaite A, Pickworth J, Lu C, Novoyatleva T, Kiely DG, Grimminger F, Ghofrani HA, Weissmann N, *et al*: Eplerenone attenuates pathological pulmonary vascular rather than right ventricular remodeling in pulmonary arterial hypertension. BMC Pulm Med 18: 41, 2018.
44. Baluk P, Yao LC, Feng J, Romano T, Jung SS, Schreiter JL, Yan L, Shealy DJ and McDonald DM: TNF-alpha drives remodeling of blood vessels and lymphatics in sustained airway inflammation in mice. J Clin Invest 119: 2954-2964, 2009.
45. Angelo LS and Kurzrock R: Vascular endothelial growth factor and its relationship to inflammatory mediators. Clin Cancer Res 13: 2825-2830, 2007.
46. Zhu G, Huang Q, Huang Y, Zheng W, Hua J, Yang S, Zhuang J, Wang J and Ye J: Lipopolysaccharide increases the release of VEGF-C that enhances cell motility and promotes lymphangiogenesis and lymphatic metastasis through the TLR4-NF-κB/JNK pathways in colorectal cancer. Oncotarget 7: 73711-73724, 2016.
47. Pham TD, Verlander JW, Wang Y, Romero CA, Yue Q, Chen C, Thumova M, Eaton DC, Lazo-Fernandez Y and Wall SM: Aldosterone regulates pendrin and epithelial sodium channel activity through intercalated cell mineralocorticoid receptor-dependent and -independent mechanisms over a wide range in serum potassium. J Am Soc Nephrol 31: 483-499, 2020.
48. Barut F, Ozacmak VH, Turan I, Sayan-Ozacmak H and Aktunc E: Reduction of acute lung injury by administration of spironolactone after intestinal ischemia and reperfusion in rats. Clin Invest Med 39: E15-E24, 2016.
49. Artunc F and Lang F: Mineralocorticoid and SGK1-sensitive inflammation and tissue fibrosis. Nephron Physiol 128: 35-39, 2014.
50. Pakshir P, Noskovicova N, Lodyga M, Son DO, Schuster R, Goodwin A, Karvonen H and Hinz B: The myofibroblast at a glance. J Cell Sci 133: jcs227900, 2020.
51. Van De Velde M, Ebroin M, Durré T, Joiret M, Gillot L, Blacher S, Geris L, Kridelka F and Noel A: Tumor exposed-lymphatic endothelial cells promote primary tumor growth via IL6. Cancer Lett 497: 154-164, 2021.
52. Sakamoto I, Ito Y, Mizuno M, Suzuki Y, Sawai A, Tanaka A, Maruyama S, Takei Y, Yuzawa Y and Matsuo S: Lymphatic vessels develop during tubulointerstitial fibrosis. Kidney Int 75: 828-838, 2009.
53. Yoshimatsu Y, Kimuro S, Pauty J, Takagaki K, Nomiyama S, Inagawa A, Maeda K, Podyma-Inoue KA, Kajiya K, Matsunaga YT and Watabe T: TGF-beta and TNF-alpha cooperatively induce mesenchymal transition of lymphatic endothelial cells via activation of Activin signals. PLoS One 15: e0232356, 2020.

This work is licensed under a Creative Commons Attribution-NonCommercial-NoDerivatives 4.0 International (CC BY-NC-ND 4.0) License.